Electrochemical properties of $LiNi_{0.5}Mn_{1.5}O_4$ cathode after Cr doping

Sung Bin Park [a], Won Sob Eom [a], Won Il Cho [b], Ho Jang [a],*

[a] *Department of Materials Science & Engineering College of Engineering, Korea University, 5-1, Anam-dong, Seongbuk-gu, Seoul 136-713, South Korea*
[b] *Eco-Nano Research Center, Korea Institute of Science and Technology 39-1, Hawolgok-dong, Seongbuk-gu, Seoul 136-791, South Korea*

Abstract

The structure and electrochemical properties of Cr doped $LiNi_{0.5-x}Mn_{1.5}Cr_xO_4$ cathodes with different Cr contents ($x = 0.00, 0.01, 0.03$, and 0.05) were investigated by X-ray diffraction, SEM, cyclic voltammetry, charge–discharge tests, and thermogravimetric analysis. In particular, restoration of Li in the cathode during intercalation was carefully analyzed by employing heating-cooling cycles of thermogravimetric technique. Results showed that the initial discharge capacity and capacity retention of the $LiNi_{0.5-x}Mn_{1.5}Cr_xO_4$ cathode were improved as the Cr content was increased. Thermal analysis and CV test results suggested that the improvement of the electrochemical properties of the Cr doped $LiNi_{0.5-x}Mn_{1.5}Cr_xO_4$ cathode was attributed to the high oxygen affinity of the Cr, which reduced oxygen deficiency and improved structural stability of the cathode.
© 2005 Elsevier B.V. All rights reserved.

Keywords: $LiNi_{0.5}Mn_{1.5}O_4$; Doping; Chromium; Lithium-ion batteries

1. Introduction

Lithium intercalated compounds have been successfully used for the cathode in the Li-batteries for several decades. Among many candidates, however, only $LiCoO_2$ cathodes have been produced in a large scale for commercial applications. This is because $LiCoO_2$ has remarkable electrochemical stability of a layered structure and is relatively easy to synthesize. However, $LiCoO_2$ has low capacity and is environmentally unfriendly and expensive. As an alternative, spinel lithium manganese oxide ($LiMn_2O_4$) has been considered as a cathode material for lithium-ion batteries since $LiMn_2O_4$ is nontoxic and cost effective. The material, however, suffers from insufficient cyclability and structural instability due to formation of impurity phases in the cathode and Jahn-Teller distortion, which reduces the capacity rapidly in the voltage range of 3–4 V [1]. The shortcomings of the $LiMn_2O_4$, however, have been improved by substituting the Mn^{3+} ion with transition metals, which provide a stronger metal–oxygen bonding [2,3].

Based on the $LiMn_2O_4$, several compounds have been developed for a cathode by the transition metal substitution and, among them, $LiNi_{0.5}Mn_{1.5}O_4$ has attracted more attention than others. This is because the $LiNi_{0.5}Mn_{1.5}O_4$ shows a dominant potential plateau around 4.7 V, while other compounds ($LiM_xMn_{2-x}O_4$, M: Cr, Co, Fe, Cu) exhibit two small plateaus at 4.0 and 5 V. Moreover, $LiNi_{0.5}Mn_{1.5}O_4$ shows the highest discharge capacity and stable cyclability at higher potentials among candidate materials [4]. The $LiNi_{0.5}Mn_{1.5}O_4$ cathode, however, shows degradation of electrochemical properties due to the Mn^{3+} ions which is closely related to the oxygen deficiency during the processing at elevated temperatures. In an ideal case of $LiNi_{0.5}Mn_{1.5}O_4$, no Mn^{3+} is present in the compound and all the Mn^{3+} ions are substituted by Ni^{2+} ions. However, a small amount of Mn^{3+} is normally left in the compound after processing at high temperature during synthesis [1]. Instead of Ni, Cr also has been employed to substitute the Mn in the $LiMn_2O_4$ to improve cycle performance and electrochemical properties. This is because Cr^{3+} ions have high oxygen affinity, providing structural stability during cycling [5–8].

In this study, we produced the Cr doped $LiNi_{0.5}Mn_{1.5}O_4$ using a sol–gel method for high voltage applications. In particular, we employed the heating–cooling cycles during thermal analysis to investigate the restoration of Li during intercalation

---

of Li, which provided the quantitative measure of the suppression of impurity phases by Cr doping during the heat treatment.

2. Experimental

$LiNi_{0.5-x}Mn_{1.5}Cr_xO_4$ ($x = 0.00$, 0.01, 0.03, 0.05) was synthesized by a sol–gel method. 1 M $(CH_3COO)Li·H_2O$, 0.5 M $(CH_3COO)_2Ni·4H_2O$, and 1.5 M $Mn(CH_3COO)_2·4H_2O$ were dissolved in distilled water and acrylic acid was added into the solution to control the reaction kinetics. $Cr(NO_3)_3·9H_2O$ was mixed in the solution to substitute Mn with Cr. Remaining water and acrylic acid were removed in a rotary evaporator at 80 °C. After drying, the product was heated for 12 h at 600 °C and it was calcined for 24 h at 800 °C under oxygen flow.

The crystal structure of the sample was examined by X-ray diffraction (D/MAX-II A) with Cu Kα with a scan range of 10–85° (2θ). To investigate thermal properties, a thermogravimetric analyzer (TGA, Netzsch STA 409EP) was carried out in the air. During TG analysis, temperature was increased at 5 °C min^{-1} to 1000 °C and decreased at −5 °C min^{-1} to 400 °C. The morphology of the powder samples was examined using an SEM (Hitachi, S-4300, Japan).

Positive electrode was prepared by combining $LiNi_{0.5-x}Mn_{1.5}Cr_xO_4$, polyvinylidene difluoride (PVdF) [5 wt% in NMP (1-methyl-2-pyrrolinone)], and carbon. The ratio was 85:5:10 in wt.%. Acetone was added to lower the viscosity before homogenizing the mixture at 5000 rpm. The cathode was cast by the Dr. blade method on an Al foil. It was pressed in a rolling press and dried in a vacuum oven for 24 h at 80 °C.

Electrochemical properties of $LiNi_{0.5-x}Mn_{1.5}Cr_xO_4$ were examined in coin cells containing a lithium foil as a negative electrode. The electrolyte was 1 M high purity $LiPF_6$ dissolved in ethylene carbonate (EC) and dimethyl carbonate (DMC) (1:2 volume ratio). Cells were assembled in a dry room and polypropylene (PP) was used for the separator. Charge–discharge experiments and cyclic voltammetry (CV) tests were carried out by using a battery cycler system (WBCS3000, Won A Tech). The charge–discharge rate was set at 1/2 C and tests were carried out for 50 cycles. The scanning rate was 0.02 mV s^{-1} and cut off voltage was in the range of 3.5–5.0 V.

3. Results and discussion

3.1. Crystal structure and surface morphology

The crystal structure and morphology of the $LiNi_{0.5}Mn_{1.5}O_4$ particles, before and after Cr-doping, was examined by XRD and SEM. Fig. 1(a) shows an XRD pattern of the bare $LiNi_{0.5}Mn_{1.5}O_4$ compound produced in this study. It showed a typical pattern of the spinel structure [9], indicating no secondary phases such as NiO and $Li_xNi_{1-x}O$ present in the compound. The XRD pattern of the Cr doped $LiNi_{0.5}Mn_{1.5}O_4$ (Fig. 1(b)) also exhibited the same spinel crystal structure (space group Fd3m) without impurity phases. The lattice parameter of the $LiNi_{0.5}Mn_{1.5}O_4$ compound was decreased (8.1785–8.1656 Å) after Cr doping ($x = 0.05$), which was attributed to the strong bonding energy of Cr with oxygen than Mn.
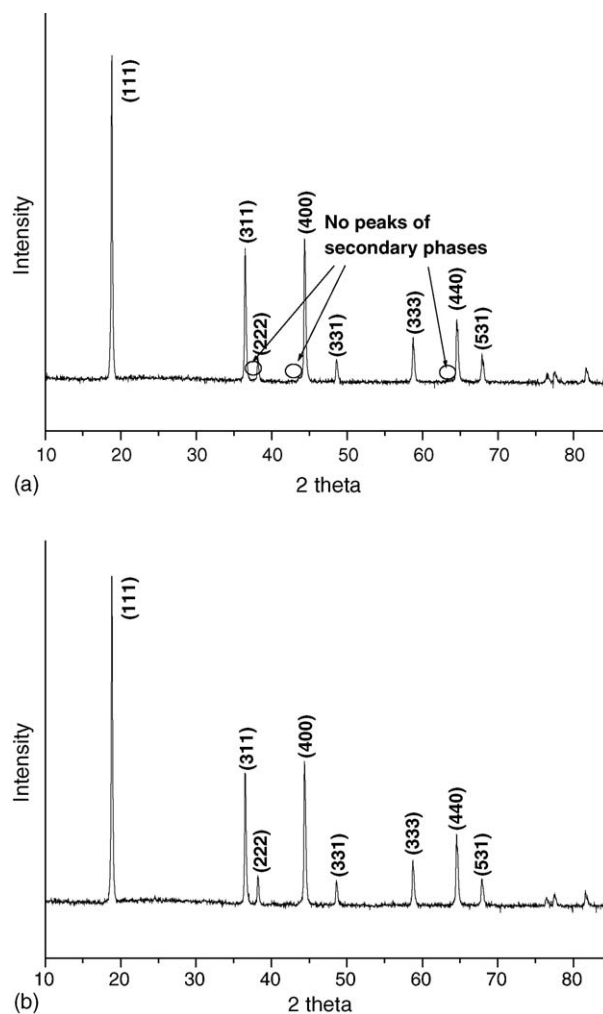

Fig. 1. The XRD patterns of $LiNi_{0.5-x}Mn_{1.5}Cr_xO_4$ (a) and $LiNi_{0.45}Mn_{1.5}Cr_{0.05}O_4$ (b). Diffraction angles (2θ) from possible impurity phases were indicated by arrows, which were not observed in our XRD patterns.

Structural stability of the $LiNi_{0.5-x}Mn_{1.5}Cr_xO_4$ was also investigated by thermal analysis. Fig. 2 shows the weight change of the cathode as a function of temperature. A large weight loss was found in the temperature range of 650–1000 °C during thermal analysis. The weight loss indicated the removal of lithium and oxygen, which led to structural transformation of the cathode [10,11]. This was because the crystal structure of $LiNi_{0.5}Mn_{1.5}O_4$ required different stoichiometry at high temperatures compared with the cathode at low temperatures since Mn^{3+} ion generation at high temperature induced oxygen deficiency in $LiNi_{0.5}Mn_{1.5}O_4$ [12,13]. The weight loss was biggest for bare $LiNi_{0.5}Mn_{1.5}O_4$ and decreased as the Cr content was increased. The recovery experiment during cooling also showed that the Cr doped $LiNi_{0.5-x}Mn_{1.5}Cr_xO_4$ restored more oxygen than the bare $LiNi_{0.5}Mn_{1.5}O_4$, implying that Cr played a crucial role in the maintenance of the oxygen in the cathode. This also supported the fact that the bare $LiNi_{0.5}Mn_{1.5}O_4$ could not maintain structural stability due to oxygen deficiency, which caused degradation of discharge capacity and poor cycle stability [8]. On the other hand, Fig. 2 showed that the Cr doped $LiNi_{0.5}Mn_{1.5}O_4$
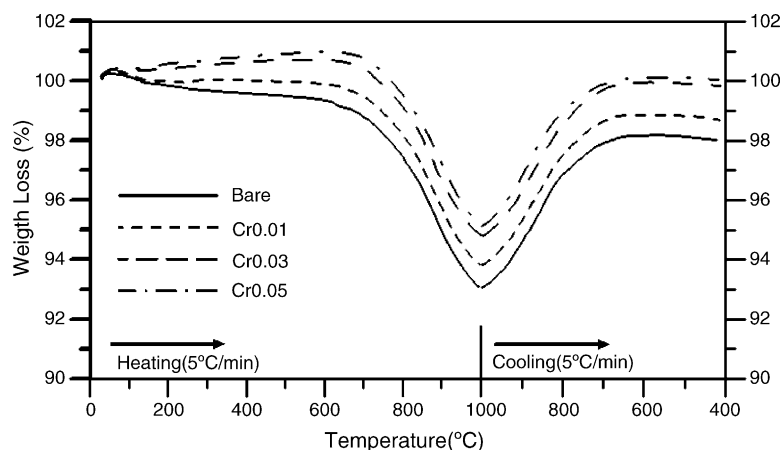
Fig. 2. TG analysis of Cr doped $LiNi_{0.5-x}Mn_{1.5}Cr_xO_4$ powders for $x = 0.00$, 0.01, 003, and 0.05.

gained its weight up to 600 °C, indicating that Cr attracted oxygen at the temperature range and the extra oxygen helped to restore the oxygen during cooling.

A similar result was reported by Thackeray et al. [14]. They found that the phase transition of $LiMn_2O_4$, from cubic to tetragonal, took place during charge–discharge experiments and it comprised the loss of both lithium and oxygen, which was similar to our current results. On the other hand, Okada et al. [15] reported a NiO secondary phase in $LiNi_xMn_{2-x}O_4$, indicating that the Ni substitution alone did not help to form stable spinel structure. It suggested that a complementary dopant was needed for synergistic effects. Hosoya et al. [8] also reported the relationship between transition metal substitution and oxygen deficiency in $LiMn_2O_4$. They showed the oxygen deficiency in the case of using Ni or Co as dopants, showing weight loss at 750 °C due to weak bonding between the two dopants and oxygen. On the other hand, it was also reported that a small amount of weight loss was observed in the case of Cr doped $LiMn_2O_4$ [6,16]. They proposed that the transition metals normally suppressed the transition of Mn^{3+} ions into Mn^{4+} ions and it reduced the Jahn-Teller distortion and enhanced structural stability.

The morphology and size distribution of the particle was also examined to study the role of Cr doping on the structural stability of $LiNi_{0.5}Mn_{1.5}O_4$. The size distribution of the particle was changed according to the Cr content and they were ranged 0.3–0.5 μm in the case of the bare material and 0.3–1.8 μm for Cr doped materials, suggesting the Cr assisted reaction kinetics. Fig. 3 also showed that the Cr doped particles exhibited surface facets during the growth of particles. Since $LiNi_{0.5}Mn_{1.5}O_4$ was a spinel in crystal structure [9], the particle tended to have an octahedral shape due to anisotropy in the surface energy [17].

3.2. Electrochemical properties

Fig. 4 shows cyclic voltammograms of bare and Cr doped $LiNi_{0.5}Mn_{1.5}O_4$. It showed several current peaks with increasing voltage, which indicated oxidation of the constituents in the cathode [18]. The peaks in the CV curve from bare $LiNi_{0.5}Mn_{1.5}O_4$ (Fig. 4(a)) corresponded to the oxidation of Mn^{3+}, Ni^{2+}, and Ni^{3+} at 4.0, 4.73, and 4.77 V, respectively. The figure indicated that the Mn^{3+} ions were present in the cathode material, which was produced during high temperature heat treatments [12,13]. The area of CV curves around 4.5–4.8 V was attributed to the amount of Ni ions involved during the electrochemical reaction, suggesting that the capacity at the high voltage was determined by the amount of Ni ions oxidized during charge–discharge experiments [19]. In the case of Cr doped $LiNi_{0.5}Mn_{1.5}O_4$ (Fig. 4(d)), the area around 4.9 V was increased when the amount of Cr was increased, suggesting the Cr oxidation in the 4.9 V range. Similar results were reported by Kawai et al. [20] and Singala et al. [21]. They reported that the capacity increase after Cr doping was attributed to the Cr^{3+} oxidation around 4.8–4.9 V. When Cr^{3+} is substituted with Ni ions in the $LiNi_{0.5}Mn_{1.5}O_4$, Mn^{3+} ions are produced in the cathode material to maintain the charge balance. However, it was reported that a small amount of Cr
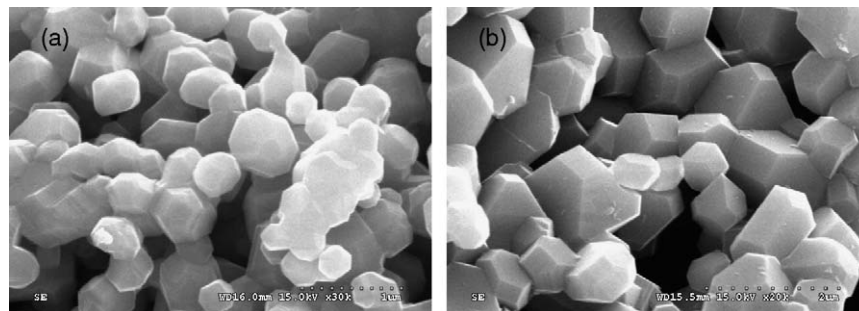

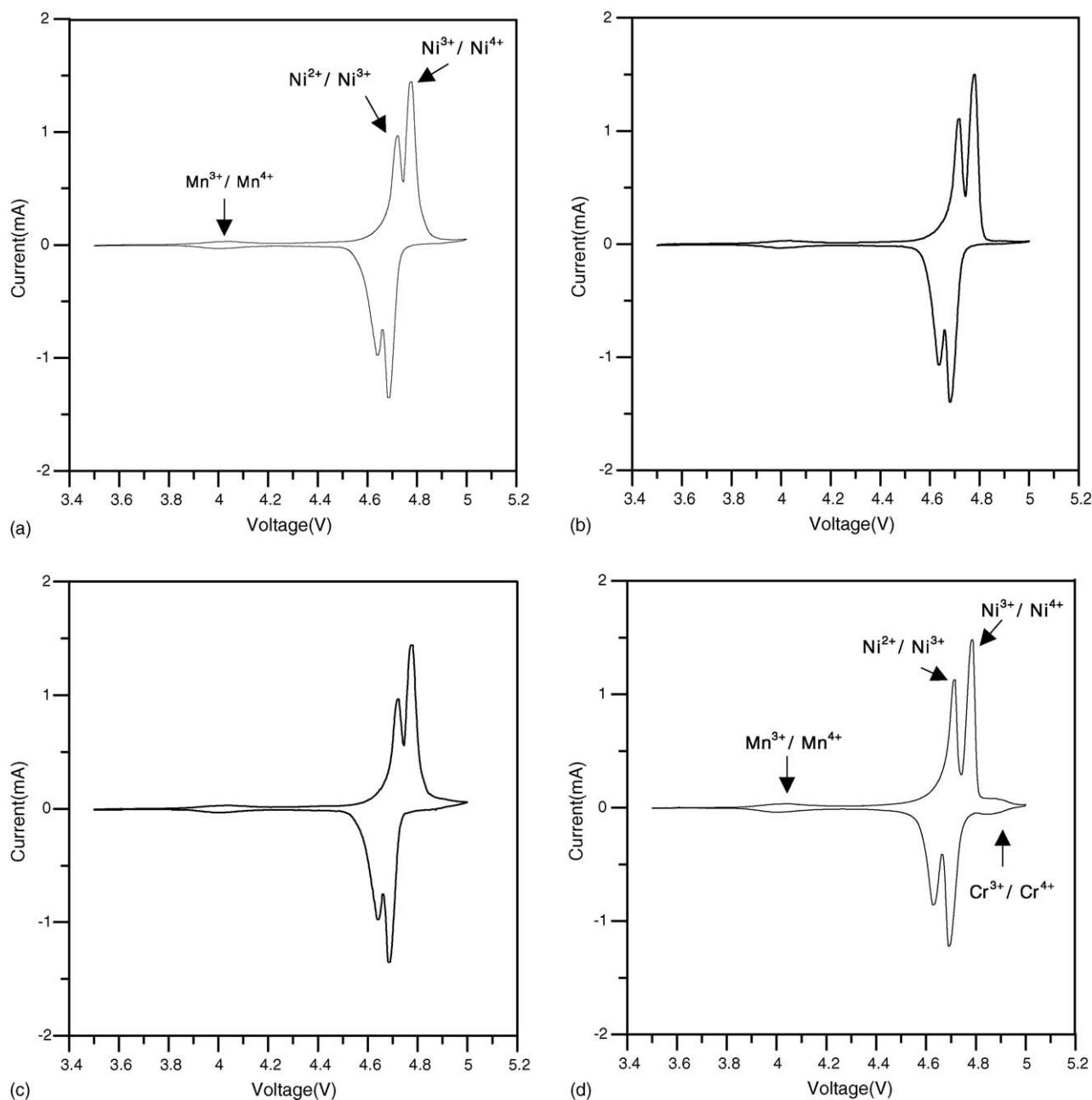Fig. 3. SEM micrographs of bare $LiNi_{0.5}Mn_{1.5}O_4$ (a) and $LiNi_{0.5-x}Mn_{1.5}Cr_xO_4$ ($x = 0.05$) particles (b).

Fig. 4. Cyclic voltammograms of $LiNi_{0.5-x}Mn_{1.5}Cr_xO_4$ powders with $x = 0.00$ (a), 0.01 (b), 0.03 (c), and 0.05 (d).

substitution suppressed Mn^{3+} generation at high temperatures and provided improved structural stability [12,13].

Charge–discharge profiles obtained from coin cells with $Li/LiNi_{0.5-x}Mn_{1.5}Cr_xO_4$ were obtained as a function of the Cr content (Fig. 5) in the $LiNi_{0.5-x}Mn_{1.5}Cr_xO_4$ cathode. The figure showed that initial capacity and capacity fading during cycling were changed when the amount of Cr doping was changed. In particular, it showed that the initial discharge capacity was increased as the Cr content increased, indicating that Cr addition stabilized the spinel structure. This was contrary to the report by Song et al. [22], which investigated the electrochemical properties of the Li-ion batteries using a $LiCr_xMn_{2-x}O_4$ cathode. They reported that the initial discharge capacity of the

$LiCr_xMn_{2-x}O_4$ was decreased during cycle tests while cyclability was improved. The initial discharge capacity from the $LiNi_{0.5-x}Mn_{1.5}Cr_xO_4$, however, was sustained well after 50 cycles when $Cr_{x=0.05}$. The figure also indicated that the two step profile of the bare $LiNi_{0.5}Mn_{1.5}O_4$ changed into nearly one step profile with a wide plateau when the Cr content was increased. Similar results were reported in the charge–discharge experiment of $LiMn_2O_4$ [23,24]. They reported that the structure of $LiMn_2O_4$ was distorted by Mn^{3+} and the capacity was reduced due to interactions between Mn^{3+} and electrolytes. A two-step profile also appeared in the case of using the bare $LiMn_2O_4$ due to Mn^{3+} oxidation and the profile was changed into a one step profile as Cr content was increased, indicating that Mn^{3+}
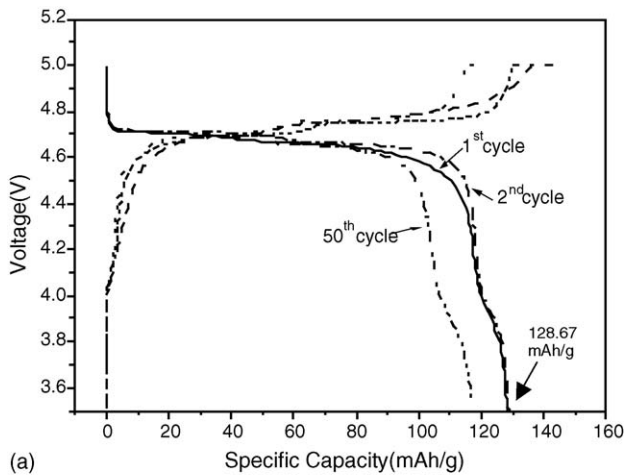
(a)
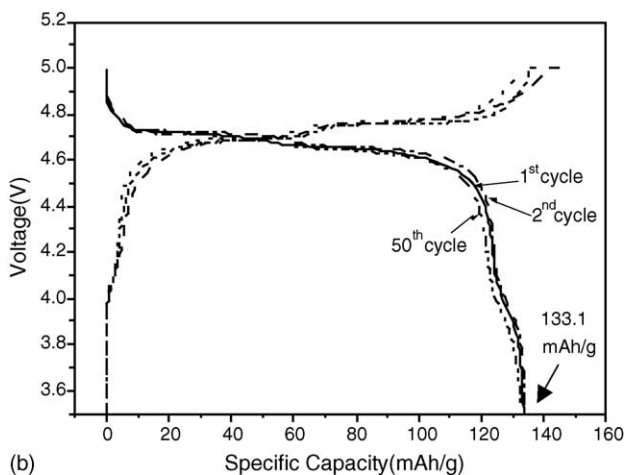
(b)

Fig. 5. Charge–discharge curves for $LiNi_{0.5-x}Mn_{1.5}Cr_xO_4$ powders for $x = 0.00$ (a) and 0.05 (b).

Fig. 6. Cycling stability curves of $LiNi_{0.5-x}Mn_{1.5}Cr_xO_4$ powders for $x = 0.00$, 0.01, 0.03, and 0.05 as a function of cycle numbers when they are tested at 1/2 C rate and in two different charge cut.

ions were suppressed by Cr^{3+} ions. The wide plateau and the high discharge capacity of the $LiNi_{0.5-x}Mn_{1.5}Cr_xO_4$ ($x = 0.05$) cathode in Fig. 5(b), therefore, appeared due to the strong chemical affinity of Cr with oxygen. It is known that small amount of Cr doping stabilizes the cathode structure and provides high capacity [25,26] while Cr addition changes the charge balance of the $LiNi_{0.5}Mn_{1.5}O_4$. They reported that the improvement of the electrochemical properties was achieved up to 0.1 mole of Cr^{+3} addition in the cathode and it was attributed to the reduction of residual Mn^{+3} remained after high temperature processing.

Fig. 6 shows capacity retention of the cathode $LiNi_{0.5-x}Mn_{1.5}Cr_xO_4$ with different Cr contents. Ideal discharge capacity of $LiNi_{0.5}Mn_{1.5}O_4$ was 149 mAh g^{-1}. However, the ideal capacity was not achieved in the charge discharge. For better understanding of the capacity in the charge–discharge process, $LiNi_xMn_{2-x}O_4$ is often expressed as $Li^{1+}Ni^{2+}{}_xMn^{3+}{}_{1-2x}Mn^{4+}{}_{1+2x}O^{2-}$ [2], assuming that Ni^{2+} replaces Mn^{3+} in the compound. In an ideal case, therefore, $LiNi_{0.5}Mn_{1.5}O_4$ without Mn^{3+} ions can be obtained because Mn^{3+} ions can be completely substituted by Ni^{+2} ions. However, when it is synthesized via conventional methods, a small amount of Mn^{3+} is normally found in the $LiNi_{0.5}Mn_{1.5}O_4$ due
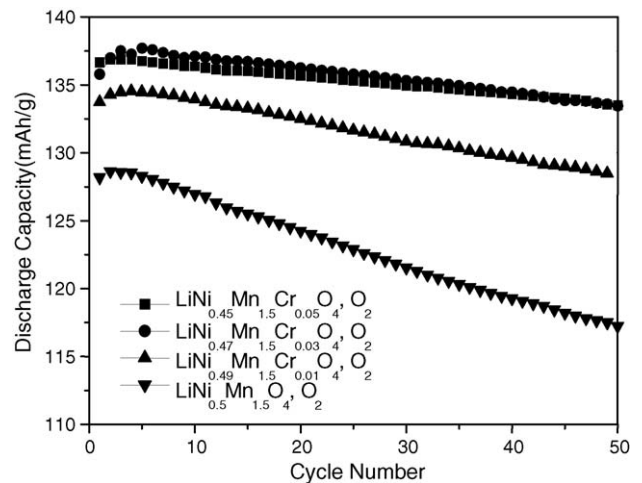
to the formation of secondary phases and oxygen deficiency during high temperature processing [2,27,28]. In our test results, initial discharge capacity of the bare $LiNi_{0.5}Mn_{1.5}O_4$ was 128.67 mAh g^{-1} and capacity retention was maintained up to 92% after 50 cycles. On the other hand, in case of Cr ($x = 0.05$) doped $LiNi_{0.5}Mn_{1.5}O_4$, initial discharge capacity was 137 mAh g^{-1} and capacity retention was maintained up to 97.5%. The differences in the capacity retention between the bare material and Cr doped materials appeared due to the high chemical affinity of Cr with oxygen, which provided excess current at the 5 V region and stable intercalation at the high voltage range [8].

4. Conclusions

The effects of Cr doping on the electrochemical properties of $LiNi_{0.5}Mn_{1.5}O_4$ were studied using electrochemical tests and several analytical methods such as XRD, SEM, and TGA. Results from this work can be summarized as follow.

(i) The spinel structure of $LiNi_{0.5-x}Mn_{1.5}Cr_xO_4$ was maintained up to $x = 0.05$ and Cr doping accelerated chemical reaction kinetics, producing well-facetted $LiNi_{0.5-x}Mn_{1.5}Cr_xO_4$ ($x = 0.05$) particles faster than others.

(ii) The amount of weight loss during TG analysis was decreased as the Cr content was increased. This suggested that the structure of the $LiNi_{0.5-x}Mn_{1.5}Cr_xO_4$ was stabilized by Cr doping due to high oxygen affinity of Cr.

(iii) Cr doping provided a wider plateau during charge–discharge tests by suppressing the Mn^{3+} oxidation, which was related to the change of the charge–discharge curves from a two step profile to a one step profile.

(iv) The initial discharge capacity of $LiNi_{0.5-x}Mn_{1.5}Cr_xO_4$ cathode was increased and capacity retention was improved with Cr content, indicating improvement of structural stability the cathode.

Acknowledgements

References

[1] Q. Zhong, A. Bonakdarpour, J.R. Dahn, J. Electrochem. Soc. 144 (1997) 205.

[2] S.T. Myoung, S. Komaba, N. Kumagai, H. Yashiro, H.T. Chung, T.H. Cho, Electrochim. Acta 47 (2002) 2543.

[3] D. Song, T. Uchida, M. Wakihara, Solid State Ionics 117 (1999) 151.

[4] T. Ohzuku, S. Takeda, M. Iwanaga, J. Power Sources 81 (1999) 90.

[5] A.D. Robertson, W.F. Howard Jr., J. Electrochem. Soc. 144 (1997) 3505.

[6] C. Sigala, A. Verbaere, J.L. Mansot, D. Guyomard, Y. Piffard, M. Tournoux, J. Solid State Chem. 132 (1997) 372.

[7] E. Iwata, K. Takahashi, K. Maeda, T. Mouri, J. Power Sources 81–82 (1999) 430.

[8] M. Hosoya, H. Ikuta, M. Wakihaha, Solid State Ionics 111 (1998) 153.

[9] X. Wu, S.B. Kim, J. Power Sources 109 (2002) 53.

[10] R. Kanno, M. Yonemura, T. Kohigashi, Y. Kawamoto, J. Power Sources 97–98 (2001) 423.

[11] T. Tsuji, H. Umakoshi, Y. Yamamura, J. Phys. Chem. Solids 66 (2005) 283.

[12] S.T. Myung, H.T. Chung, J. Power Sources 84 (1999) 32.

[13] S.T. Myung, S. Komaba, N. Kumagai, H. Yashiro, Electrochim. Acta 47 (2002) 2543.

[14] M. Thackeray, M.F. Mansuetto, J.B. Bates, J. Power Sources 68 (1997) 153.

[15] M. Okada, Y.S. Lee, M. Yoshio, J. Power Sources 90 (2000) 196.

[16] Y.C. Su, Q.F. Zou, Y.U. Wang, P. Yu, J.Y. Liu, Mater. Chem. Phys. 84 (2004) 302.

[17] M.R. Huang, C.W. Lin, H.Y. Lu, Appl. Surf. Sci. 177 (2001) 103.

[18] Y. Gao, J.R. Dahn, Phys. Rev. B 54 (1996) 16.

[19] Y.K. Sun, C.S. Yoon, I.H. Oh, Electrochim. Acta 48 (2003) 503.

[20] H. Kawai, M. Nagata, H. Tukamoto, A.R. West, J. Power Sources 81–82 (1999) 67.

[21] C. Sigala, D. Guyomard, A. Verbaere, Y. Piffard, M. Tournoux, Solid State Ionics 81 (1995) 167.

[22] G.M. Song, Y. Zhou, Y. Zhou, J. Power Sources 128 (2004) 270.

[23] K. Miura, A. Yamada, M. Tanaka, Electrochim. Acta 41 (1996) 249.

[24] Y. Ein-Eli, R.C. Urian, W. Wen, S. Mukerjee, Electrochim. Acta 50 (2005) 1931.

[25] M. Yoshio, Y. Xia, N. Kumana, S. Ma, J. Power Sources 01 (2001) 79.

[26] K. Hong, Y.K. Sun, J. Power Sources 109 (2002) 427.

[27] J.M. Tarascon, W.R. McKinnon, F. Coowar, T.N. Bowmer, G.G. Amatucci, D. Guyomard, J. Electrochem. Soc. 141 (1994) 1421.

[28] A. Yamada, M. Tanaka, J. Elecrtochem. Soc. 142 (1995) 2149.